Water and Climate
in the Western United States

Edited by William M. Lewis Jr.

Use of Weather and Climate Information in Forecasting Water Supply in the Western United States

FIVE

MARTYN P. CLARK
LAUREN E. HAY
GREGORY J. MCCABE
GEORGE H. LEAVESLEY
MARK C. SERREZE
ROBERT L. WILBY

Water in the West is allocated among diverse uses and is subject to mounting demand caused by a growing population and changes in institutional practices (Pulwarty 1995; Diaz and Anderson 1995). Demand coupled with climate variability and potential climate change presents formidable challenges for water managers. For example, the U.S. Bureau of Reclamation has indicated that if the West were to experience a drought similar to that of 1931–1940, the water needs of the lower Colorado River basin would not be met (el-Ashry and Gibbons 1988). These concerns have stimulated attempts to develop better water-management tools and improved information on snowpack. A key goal is to improve hydrologic forecasts.

Currently, hydrologic forecasts are made with the extended streamflow prediction (ESP) procedure (Day 1985). ESP is based on a hydrologic model that is calibrated with observed precipitation and temperature data up to the beginning of the forecast interval and then run with an ensemble of temperature and precipitation data from every past year in the historical record. The model thus provides an ensemble of possible outcomes given the antecedent conditions (e.g., soil moisture, water equivalent of the accumulated snowpack) at the start of the forecast. Because the methodology of ESP weights equally the history of each past year, it yields a wide range of possible outcomes.

Although advances in climate research in recent decades have led to potentially useful weather predictions and climate outlooks (e.g., Kalnay et al. 1998; Barnston et al. 2000), this information is not used in ESP modeling. The use of historical data in ESP modeling means that accuracy of the forecasts is entirely dependent on the effect of basin initial conditions on future runoff. Replacing the ensemble of historical data used in ESP modeling with an ensemble of weather forecasts and climate outlooks (i.e., using weather forecasts and climate outlooks as input to hydrologic models) may reduce the range of possible outcomes and increase the accuracy of hydrologic forecasts.

This chapter examines ways in which information on weather and climate can be useful in managing water resources in the western United States. We focus on two timescales of variability. On intraseasonal timescales (1–2 weeks) we examine the possible use of output from global-scale atmospheric forecast models in generating short-term streamflow forecasts. On seasonal timescales we assess the role of El Niño and La Niña events in shaping the seasonal snowpack, which may then be used in forecasting seasonal hydrology.

INTRASEASONAL HYDROLOGIC FORECASTS

This section addresses the hypothesis that coupling short-range atmospheric forecast models with hydrologic models can improve upon the traditional ESP methods (e.g., Day 1985). As a demonstration of this approach, over 2,500 individual eight-day forecasts from the National Center for Environmental Prediction (NCEP) reanalysis project (described later) are used as input to the U.S. Geological Survey's (USGS) Precipitation Runoff Modeling System (PRMS) to forecast stream flow in the Animas River basin in southwestern Colorado (Figure 5.1). The Animas River basin has a drainage area of 1,820 km^2 at elevations that range from 2,000 to 4,000 m. The surface hydrology of the Animas River basin is dominated by snowmelt, which is typical of most small basins in the mountainous areas of the continental western United States. This basin therefore provides a good test of the feasibility of using atmospheric forecasts for predicting runoff in that region.

NCEP Reanalysis

The NCEP reanalysis project (Kalnay et al. 1996) produced a fifty-one-year (1948–1998) record of global atmospheric fields derived from a Numerical Weather Prediction model that was kept unchanged over the analysis period. Use of fixed conditions in the reanalysis eliminates pseudoclimatic jumps in the climate time series caused by upgrades in the modeling system used at NCEP, thus allowing for assessment and correction of systematic problems in the model. The model used for reanalysis is identical to the Medium Range Forecast model implemented operationally at NCEP in January 1995 (Basist and Chelliah 1997), except that the horizontal resolution is twice as coarse in the reanalysis version. The model employs a horizontal grid spacing of approximately 210 km. Every five days during the 1948–1998 period, a single realization of an eight-day atmospheric forecast was run, and the output was archived along with the standard (day zero) reanalysis output. This procedure provides over 2,500 eight-day forecasts that can be compared with observations.

The USGS Precipitation Runoff Modeling System

The PRMS hydrologic model (Leavesley at al. 1983; Leavesley and Stannard 1995) is a distributed-parameter, physical watershed model. Parameters are spatially distributed on the basis of hydrologic response units (HRUs), which are distinguished on the basis of characteristics such as slope, aspect, elevation, vegetation type, soil type, and distribution of precipitation. A typical area for an HRU is 5 km^2. Each HRU is assumed to be homogeneous in its hydrologic response. The PRMS model generally is run with daily data on precipitation and maximum and minimum temperature, which are available for most climate stations across the United States.

Because the station network in the Animas Valley is not dense enough to allow direct measurements on each individual HRU, the daily values at meteorological stations within and around the valley (Figure 5.1) are distributed to the HRUs within the basin. To achieve this, latitude (x), longitude (y), and elevation (z) were used as independent variables in a multiple linear regression (MLR) model to establish the influence of each station on mean spatial variations in precipitation and maximum and minimum temperature throughout the basin. Use of the station x and y coordinates in the regression model provides information on the local-scale influences on precipitation and temperature that are not related to elevation (for example, distance to a topographic barrier). Daily mean values of precipitation and maximum and minimum temperature, as calculated from a subset of stations in the region, are then used with the xyz MLR relations to distribute precipitation and temperature over the basin according to the mean values of x, y, and z for each HRU. A separate regression model was developed for each month to account for seasonal variations in the relationships of topography with precipitation and temperature. The distributed data are used to compute an energy and water balance for each HRU. The sum of the water balances of each HRU, weighted by unit area, produces the daily watershed response. In basins the size of the Animas (1,820 km^2), the travel of water through the channel network typically occurs on timescales of less than one

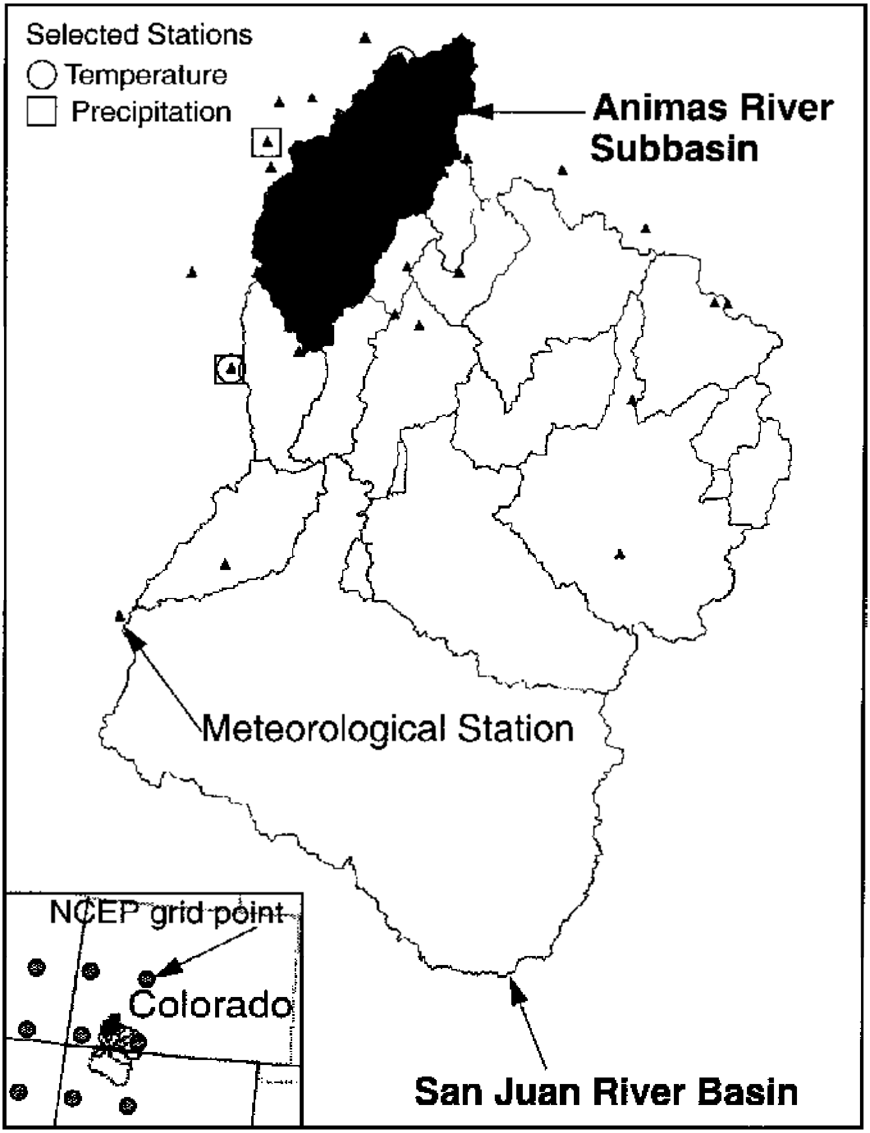

5.1 Map showing the meteorological station network (small triangles) of the San Juan River basin and the Animas River subbasin, Colorado. Locations of stations providing temperature data (circles) and precipitation data (squares) for modeling are shown.

day. For this reason, we chose not to include flow routing routines in our hydrologic simulations.

Snow is the major form of precipitation and source of stream flow in the Animas River basin. PRMS simulates the accumulation and depletion of a snowpack on each HRU. Snowpack is maintained and modified as both a water reservoir and a dynamic heat reservoir. Snowmelt does not occur until the snow surface temperature warms to 0°C, and outflow at the base of the snowpack does not occur until the entire snowpack warms to 0°C. A water balance is computed daily, and an energy balance is computed twice each day. Lack of data on wind speed, humidity, and radiation means that the energy balance computations must be greatly simplified. These computations include estimates of incoming shortwave and longwave radiation and the heat content of precipitation. The turbulent heat transfers of latent and sensible heat are approximated. Solar radiation is distributed to each HRU on the basis of slope and aspect. Neither shortwave nor longwave radiation is measured at the climate stations in this region, so these variables are estimated from their empirical relationships with temperature and precipitation.

Precipitation and snowmelt ultimately reach the channel network through surface runoff, subsurface flow, or groundwater. The first opportunity for precipitation and snowmelt to generate stream flow is via surface runoff, which takes place if the net water input exceeds the infiltration capacity of the soil over the entire HRU or if some areas of an HRU become completely saturated (this typically arises in lower regions of an HRU where topography causes an accumulation of water). PRMS simulates both of these processes. In the Animas River basin the combination of highly pervious soils (maximum infiltration rate is assumed to be 50 mm/day) and moderately low daily precipitation and snowmelt means that only a small fraction of the basin area is completely saturated. Thus contributions from surface runoff are small, and almost all runoff in the Animas River basin is derived from subsurface and groundwater flow.

The dominance of subsurface flow results in a time lag between surface-water inputs and the hydrologic response of the basin. In the PRMS model, water percolates to deep soil zones and groundwater reservoirs after the water-holding capacity of the upper soil layer is exceeded. Water recharges the groundwater reservoir at an assumed rate of 3 mm/day. Water in excess of this rate becomes inflow to the subsurface, which drives subsurface flow. Subsurface flow is the rapid movement of water through the matrix and preferential flow paths composing the soil and unsaturated-zone profile to the stream channel. Subsurface flow increases nonlinearly with the amount of water stored in the subsurface reservoir. The response time of the catchment is therefore faster if subsurface storage is high. For hydrologic forecasting, accurate initialization of subsurface conditions is important. Base flow from the groundwater reservoir is computed as a linear function of groundwater storage and occurs on timescales of days to weeks, thus introducing additional lags into the hydrologic system.

Hydrologic Forecast Procedures

Assuming a perfect hydrologic model, the accuracy of hydrologic forecasts depends on the skill of atmospheric forecasts and the accuracy with which initial conditions can be specified over the basin. The most important initial conditions for hydrologic forecasts are the water equivalent of snow and the soil moisture on each HRU and the amount of water stored in the subsurface and groundwater reservoirs. We establish these initial conditions by forcing PRMS with distributed station observations of precipitation and maximum and minimum temperature for the time period of the NCEP reanalysis, starting three years prior to the day before the first forecast date. The state variables (e.g., water equivalent of snow, soil moisture, subsurface storage) are saved for every five days and then used as initial conditions for the eight-day forecasts.

The hydrologic simulations obtained with distributed station data are used to assess the accuracy of the hydrologic forecasts. Taking modeled values as truth assumes a perfect hydrologic model and allows us to focus attention on hydrologic effects of errors in the atmospheric forecasts. If observed runoff is used as truth, situations may arise for which errors in the atmospheric forecasts are of opposing sign to errors in the hydrologic model simulations, thus tending to cancel them. This would provide a misleading perception of reliability for the hydrologic forecasts.

Following the simulations of runoff based on station data, two hydrologic forecast experiments were performed. In the first experiment, eight-day hydrologic forecasts were run using constant precipitation and maximum and minimum temperatures computed from historical station data for each forecast period. This is termed the climatology experiment. It provides output analogous in many respects to the mean response in ESP simulations and quantifies the skill that is possible when forecasts are based on historical station data. The second experiment forces the PRMS hydrologic modeling system with the eight-day forecasts of precipitation and maximum and minimum temperature from an average of the nine NCEP model grid points surrounding the Animas River basin. This is termed the forecast experiment.

At the NCEP model grid points overlying the Animas basin, the raw NCEP forecasts show systematic biases in predicting temperature and precipitation. Winter and spring temperatures are too low, summer temperatures are too high, precipitation in late winter is too high, and precipitation in summer and early autumn is too low. These biases are markedly different at various forecast lead times (i.e., biases for one-day forecasts differ from the hydrology of the Animas River basin. Runoff is highest and most variable in May and June.

Hydrologic Forecasts Using Climatology

In the climatology experiment, forecast errors in maximum and minimum temperatures and precipitation are similar for different forecast lead times because these variables are set to constant mean values on the basis of historical data for each forecast period. The small changes in error with forecast time occur because, with the forecast runs spaced five days apart, different data are used to verify forecasts at different lead times. Forecasts of snowmelt, actual ET, and runoff, as computed by the model, were lowest at the start of the forecast cycle because of the influence of initial conditions on forecasts. To facilitate direct comparison with the NCEP forecasts, the climatological forecasts were run every five days. Results for the climatology experiment are presented in the left column of Plate 11.

Hydrologic Forecasts With NCEP Output

The accuracy of the forecasts based on output from the NCEP model is presented in the middle column of Plate 11. The right column is the difference between the forecast and the climatology experiment (middle column subtracted from the left column) and represents the improvement provided by using forecasts instead of climatology.

Only in some cases is the accuracy of the NCEP forecasts superior to that of forecasts based on climatology (middle and right columns of Plate 11). Generally, forecast accuracy is limited by the coarse horizontal resolution of the NCEP model (for example, precipitation varies on the subgrid scale) and deficiencies in modeling of physical phenomena. For example, summer precipitation may be poorly represented because of inadequacies in parameterization of convective processes. The poor forecasts of precipitation limit the use of output for river basins where the surface hydrology is dominated by rain. In snowmelt-dominated river systems typical of the western United States, however, short-term variation in runoff is influenced more by variation in temperature than by variation in precipitation. Thus accurate hydrologic predictions are more likely. In the Animas River basin, because the highest accuracy in forecasts of maximum temperature coincides with the spring melt (Plate 11), accurate predictions of runoff are feasible.

Improvements in the modeled variables through use of NCEP forecasts are readily apparent from the last three graphs of the right column in Plate 11. During the spring melt period, errors in forecasts of snowmelt are low for the first four days of the forecast cycle because of the high accuracy in forecasts of maximum temperature for March, April, and May. Likewise, reductions in forecast errors of actual ET are evident in late spring. In midsummer,

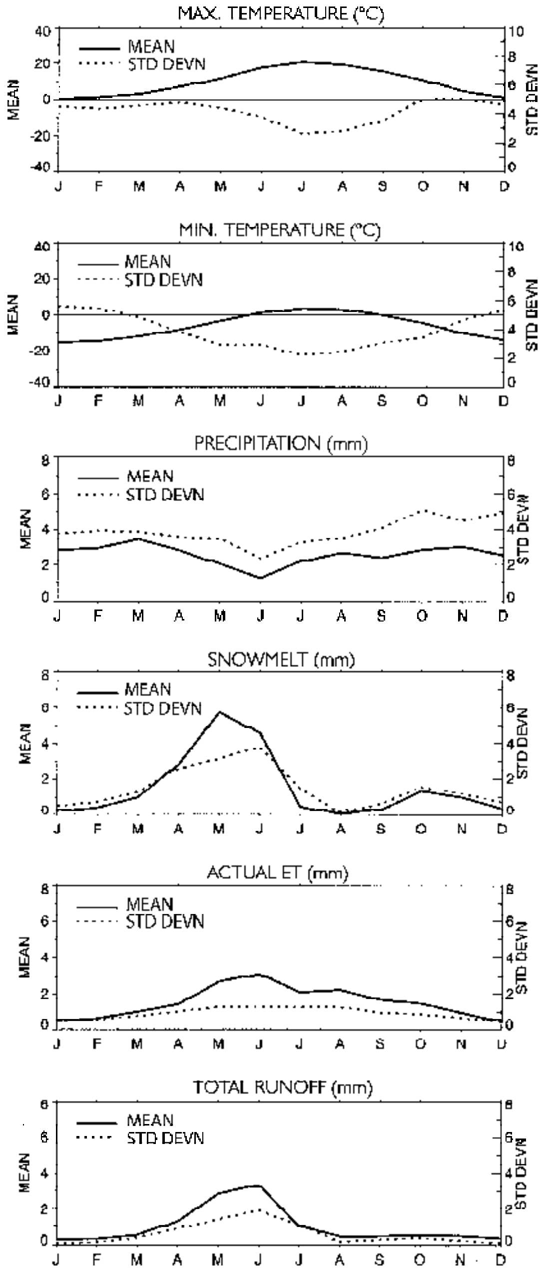

5.2 Seasonal cycles of the long-term monthly mean and daily standard deviation of maximum and minimum temperature and precipitation (inputs to PRMS-distributed hydrological model; see text) as well as snowmelt, actual evapotranspiration (ET), and total runoff (PRMS model outputs) for the Animas basin.

biases for eight-day forecasts). As a pre-processing step, we removed all systematic biases before the NCEP forecasts were used in the PRMS hydrologic modeling system. Biases in maximum and minimum temperatures were removed by computing a monthly climatology of the NCEP temperatures for each forecast lead time, subtracting the forecast value from that climatology (to produce a daily anomaly value), and adding the daily anomaly to the corresponding monthly station climatology of maximum and minimum temperature. Because precipitation data are not normally distributed, correcting for constant bias over the entire data range is not valid. To circumvent this problem, we classified the precipitation data by deciles and performed the bias correction outlined earlier independently for each decile. The bias corrections only apply to systematic biases in the NCEP fields; they do not account for biases associated with specific weather regimes (e.g., precipitation may be underestimated during the passage of a cold front and overestimated when high pressure is dominant). The bias corrections are possible only because the NCEP model was held constant throughout the reanalysis period. In an operational setting the model is frequently upgraded, and such corrections (as well as more sophisticated statistical procedures such as statistical downscaling) are not possible.

Surface-Water Hydrology of the Animas River Basin

Monthly variations in the mean and standard deviation of the three variables used as input to PRMS (maximum and minimum temperatures and precipitation) and of the three modeled variables (snowmelt, actual evapotranspiration [ET], and runoff) are presented in Figure 5.2. Figure 5.2, which is based on the simulations using station data, describes the influence of precipitation and temperature on the hydrology of the Animas River basin, as well as seasonal variations in the hydrologic response of the basin. Temperatures reflect the midlatitude, continental location of the region. Mean maximum temperatures are close to 0°C from November to March, and minimum temperatures are below freezing most of the year. Temperatures rise significantly in summer months, when mean basin-average maximum temperatures are close to 20°C. Both minimum and maximum temperatures are most variable in winter months. Precipitation is relatively constant across seasons but tends to be low in early summer and high during autumn. Most winter precipitation falls as snow and is stored in the snowpack until spring. Modeled snowmelt is highest and most variable in April, May, and June. Although temperatures are generally too low for melt to occur in midwinter, a secondary melt occurs in October and November when snow cover is transient. Actual ET is highest throughout the summer, especially in May and June, when the amount of soil moisture is high. The seasonal cycle of runoff is similar to that of snowmelt, illustrating the importance of snow for the however, NCEP forecasts of ET are less accurate than forecasts of ET based on climatology. This is consistent with the poor forecast accuracy for maximum temperature at this time of year. In terms of runoff, reductions in forecast errors during the spring melt period are remarkable. Forecast errors at the end of the forecast period (seven to eight days) are almost halved when the hydrologic model is forced with the NCEP output. Forecast accuracy for runoff at such long lead times exceeds the forecast accuracy for maximum temperature and snowmelt because of the natural lags and integrating effects of hydrologic systems.

Summary and Discussion

The NCEP atmospheric model, when coupled with the PRMS-distributed hydrologic model, provides forecasts of runoff with errors much lower than those of hydrologic forecasts based on climatology. In addition, accuracy of runoff forecasts is evident at longer lead times (about four days) than for the forecasts of maximum temperature and snowmelt because of the natural lags and integrating effects of hydrologic systems, particularly with regard to subsurface flow. Greater accuracy at longer lead times underscores the importance of specifying initial conditions accurately over the basin at the start of the forecast period. Although we do not currently assimilate satellite data into the hydrologic modeling, we anticipate that in the future satellite data will provide more accurate estimates of initial conditions for hydrologic forecasts.

The accuracy of runoff forecasts in this study is possible because the hydrology of the Animas River basin is dominated by snowmelt, which is influenced predominantly by temperature. In other river basins where the hydrology is more heavily influenced by rainfall, the accuracy of precipitation forecasts will be more important. Because the precipitation forecasts from global-scale models are rather poor (particularly on the small spatial scales used in hydrologic applications), use of raw, global-scale forecasts is unlikely to provide reliable forecasts of runoff for rainfall-dominated hydrologic systems. In the Animas River basin, skillful predictions of maximum temperature happen to coincide with the timing of snowmelt. Predictions of maximum and minimum temperatures do not improve upon climatology during summer, and predictions of maximum temperature are little better than climatology in winter.

Because some of the largest forecast errors can be attributed to the coarse horizontal resolution of the NCEP model, it may be prudent to explore methods that resolve subgrid-scale information in the forecast fields by statistical downscaling through the use of Model Output Statistics (MOS; Wilks 1995; Wilby et al. 1999). MOS is based on empirical relations between features reliably simulated as global-scale forecast models at grid-box scales (e.g., 500 hectoPascals [hPa] geopotential height) and surface characteristics at subgrid scales (e.g., occurrence and amount of precipitation). An alternative approach is through dynamical downscaling, whereby a dynamically based regional-scale climate model is nested within the global-scale forecast model. Although the computational requirements of such an approach are demanding, rapid increase in computer power over the past decade has allowed regional climate models to become a major tool in short-term numerical weather prediction. Comparisons of ten years of dynamically downscaled NCEP output from the RegCM2 regional climate model run at a horizontal resolution of 50 km, and statistically downscaled NCEP output using MOS for simulating the surface hydrology of the Animas River basin shows that the statistical approach performs slightly better than the dynamical approach (Wilby et al. 2000) or the raw NCEP output. Because precipitation and temperature variations often occur on spatial scales much smaller than 50 km, however, it may be premature to rule out the utility of regional climate models. It is likely that nesting a series of regional climate models to scales of less than a square kilometer is necessary to resolve adequately the subgrid-scale variations important for hydrologic modeling.

SEASONAL HYDROLOGIC FORECASTS

At seasonal timescales, predictive skill can be derived from knowledge of ways in which the slowly varying components of the climate system (e.g., tropical sea-surface temperatures, continental soil moisture, and albedo) alter the probability of extremes in precipitation and temperature. In the snow-fed river systems of the western United States, many water-management decisions are based solely on the amount of water stored in the seasonal snowpack at various times during the accumulation season, whereas relatively little attention is paid to mechanisms by which low-frequency climate variations may influence patterns of snow accumulation. One of the most widely studied low-frequency variations in the climate system is the El Niño–Southern Oscillation (ENSO). Here we focus on the Columbia and Colorado River basins and show how El Niño and La Niña events modulate the seasonal evolution of the montane snowpack in these basins.

Effects of ENSO on Western Water Resources

The El Niño–Southern Oscillation describes quasi-periodic variations in sea-surface temperature (SST) of the tropical Pacific Ocean and associated pressure oscillations between Tahiti and Darwin, Australia (Rasmusson and Wallace 1983; Chapter 1). El Niño (warm) events are characterized by above-normal SSTs in the eastern tropical Pacific Ocean and increased convection and precipitation near and east of the International Dateline. During La Niña (cold) events, SST anomalies generally oppose those of El Niño events,

Table 5.1—Years ranked in terms of the magnitude of the Niño 3.4 index (area-averaged SST over the region 120°W–170°W, 5°S–5°N) and the Southern Oscillation Index (sea-level pressure difference between Tahiti and Darwin). The SOI was multiplied by –1, which makes it ordinally consistent with the Niño 3.4 index. The years are defined as the date at the end of winter (i.e., the winter of 1982–1983 is taken as 1983).

Rank	*Index NINO3.4*	*Index SOI*	*Rank*	*Index NINO3.4*	*Index SOI*	*Rank*	*Index NINO3.4*	*Index SOI*
1	1989	1974	17	1963	1957	32	1978	1959
2	1974	1971	18	1962	1984	33	1980	1981
3	1971	1989	19	1981	1961	34	1952	1994
4	1976	1976	20	1961	1968	35	1964	1969
5	1956	1956	21	1957	1986	36	1977	1995
6	1985	1951	22	1960	1954	37	1988	1973
7	1955	1967	23	1990	1979	38	1970	1952
8	1996	1962	24	1982	1977	39	1995	1990
9	1951	1963	25	1979	1965	40	1969	1958
10	1984	1960	26	1994	1964	41	1966	1966
11	1975	1955	27	1954	1988	42	1987	1993
12	1968	1975	28	1953	1991	43	1973	1978
13	1965	1982	29	1991	1970	44	1958	1987
14	1986	1985	30	1993	1980	45	1992	1992
15	1967	1972	31	1959	1953	46	1983	1983
16	1972	1996						

Southern Oscillation Index for the Niño 3.4 index (Table 5.1) and by varying the number of years designated as El Niño or La Niña events.

Computing Basinwide Estimates of SWE

Basinwide estimates of SWE were computed for each of the major subbasins in the Columbia and Colorado watersheds. This was done using snowcourse measurements taken on or near February 1, March 1, April 1, and May 1 for all years between 1951 and 1996. Snowcourses were assigned to drainage basins by use of hydrologic unit codes (Seaber et al. 1987). For the Columbia River, the relevant subbasins within the United States are the upper Columbia and Yakima, Pend Oreille and Kootenai, Snake River, and lower Columbia (Figure 5.3). The relevant subbasins in the Colorado River basin include the upper Green; the Colorado headwaters, the White River, and the Yampa; the lower Green and Lake Powell; the San Juan, Gunnison, and Dolores Rivers; and the lower Colorado (Figure 5.3). Descriptions of these basins are provided in Table 5.2.

ENSO-SWE Associations for the Columbia River Basin

Composite anomalies and inter-ENSO variability in SWE for the subbasins in the Columbia River are illustrated in Figure 5.4. The bars represent the maintained by the United States Department of Agriculture's cooperative snow survey program. The program is coordinated by the Natural Resources Conservation Service, which has partners conducting measurements in Arizona, Colorado, Idaho, Montana, Nevada, New Mexico, Oregon, Utah, Washington, and Wyoming. In addition, the California Department of Water Resources has an independent program. The number of snowcourse locations grew from fewer than 10 in the 1910s to almost 2,000 in the 1970s. Snowcourse measurements decreased in the 1980s and 1990s as a result of the development of the automated Snowpack Telemetry (Snotel) system (Serreze et al. 1999). SWE is generally measured on or about the beginning of each month from January through June. Additional measurements may be taken in the middle of the month if knowledge of snowpack conditions is deemed critical. Snowcourse measurements are most frequently taken at the beginning of April, which is the peak for SWE in much of the West. The frequency and timing of measurements vary considerably with the locality, the nature of the snowpack, difficulty of access, and cost (NRCS 1988).

Snow depth and SWE are measured by pushing a tube through the snowpack to the ground surface and extracting a core. SWE is determined by weighing the tube with its snow core and subtracting the weight of the empty tube. Between five and ten cores are taken at regular intervals along each snowcourse site. An average of all samples for a site is the SWE value for that site. Generally, courses are about 300 m long and are situated in small meadows protected from the wind (NRCS 1988). Possible problems with snowcourse measurements include changes in vegetation, which may change patterns of snow accumulation along the snowcourse, and errors in data entry. For present purposes, quality control of the data involves only removal of obviously impossible cases in which snowpack depth was reported as being less than its water equivalent. The effects of remaining errors are reduced through our use of basinwide SWE averages (described later).

Definition of El Niño and La Niña Events

The first step in our analysis is to identify El Niño and La Niña events. Any such classification is somewhat arbitrary. Our definition is based on mean winter (November through April) values of the Niño 3.4 index, which is the average SST anomaly in the central equatorial Pacific Ocean (5°N–5°S; 120°W–170°W), where tropical convection is most sensitive to SST variations (Hoerling et al. 1997; Trenberth 1997). Each year over the period 1951–1996 was ranked in terms of the mean wintertime anomaly value (Table 5.1). The ten warmest and ten coldest years were extracted for analysis. Attention is restricted to years after 1951, as the SST data for earlier years are somewhat unreliable. Sensitivity tests were conducted by substituting the but the negative anomalies in tropical convection and precipitation are of small magnitude and do not extend as far east as the positive anomalies of El Niño (Hoerling et al. 1997). The tropical anomalies perturb midlatitude atmospheric circulation patterns. During warm events, enhanced tropical convection results in intensification of the Hadley circulation and a strengthening and eastward extension of the Pacific subtropical jet. This is associated with a deepening of the Aleutian Low in the North Pacific Ocean and amplification of the northern branch of the tropospheric wave train over North America, resulting in a characteristic "split flow" (e.g., Bjerknes 1969; Horel and Wallace 1981; Rasmusson and Wallace 1983). The midlatitude response to cold events generally involves weakening of the subtropical jet and damping of the wave train over North America. Because of the lack of symmetry in tropical convection patterns between warm and cold events, however, sea-level pressure and anomalies at 500 hPa height during warm events are shifted, on average, 35° east of those in cold events (Hoerling et al. 1997).

In an analysis of hydrologic effects of ENSO over the western United States, Cayan and Webb (1992) computed correlations between the Southern Oscillation Index (SOI)—a simple measure of the phase and strength of ENSO—and April 1 snow-water equivalent (SWE) and between the SOI and annual runoff. They showed that SWE and annual runoff are positively correlated with the SOI in the northwestern United States but are negatively correlated with the SOI in the southwestern United States. This suggests that El Niño events lead to decreased SWE and annual runoff in the Northwest and to increased SWE and annual runoff in the Southwest and that La Niña events have the opposite effects. Other studies provide similar findings (Cayan and Peterson 1990; Koch et al. 1991; Redmond and Koch 1991; Cayan 1996). In El Niño years the amplified northern branch of the wave train over North America is associated with higher temperatures over the northwestern United States and Canada and a northward shift of the storm track toward Alaska, which decreases mean precipitation over the Pacific Northwest. To the south, the strengthened subtropical jet entrains more moisture from the Pacific Ocean, which, when combined with the increased cyclonic shear on the jet's poleward flank, increases the likelihood of precipitation over the southwestern United States. In La Niña years the stronger zonal flow allows more storm systems to penetrate into the northwestern United States, resulting in increased precipitation over this area. Over the southwestern United States, the weakened subtropical jet decreases the likelihood of precipitation.

Data

We base our analysis on SWE data collected manually on a monthly basis during winter and spring at several hundred permanent snowcourses

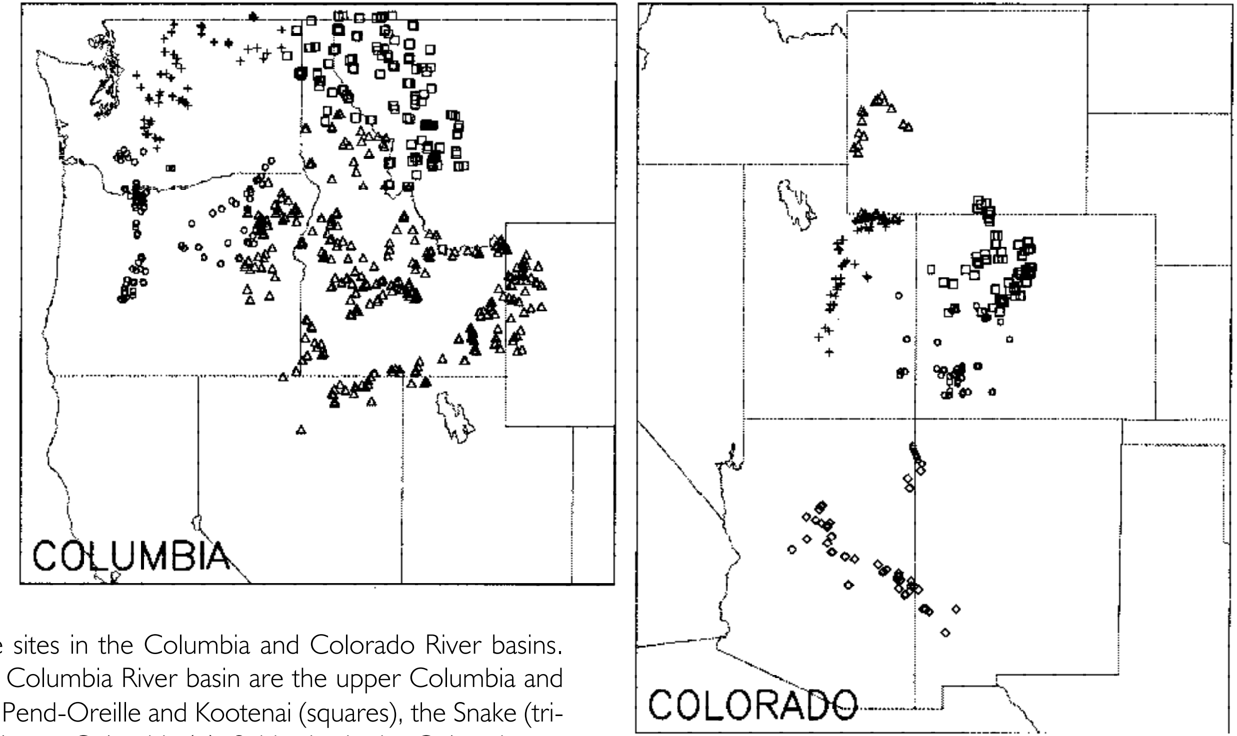

5.3 Snowcourse sites in the Columbia and Colorado River basins. Subbasins in the Columbia River basin are the upper Columbia and Yakima (+), the Pend-Oreille and Kootenai (squares), the Snake (triangles), and the lower Columbia (o). Subbasins in the Colorado are the upper Green (triangles), the Colorado headwaters (squares), the lower Green (+), the San Juan (o), and the lower Colorado (diamonds).

Table 5.2—Description of subbasins selected for this study (from Seaber et al. 1987).

COLUMBIA RIVER BASIN

UPPER COLUMBIA AND YAKIMA

Subregion 1702: Columbia River basin within the United States above the confluence with Snake River basin, excluding Yakima River basin

Subregion 1703: Yakima River basin

PEND OREILLE AND KOOTENAI

Subregion 1701: Kootenai, Pend Oreille, and Spokane River basins within the United States

SNAKE

Subregion 1704: Upper Snake: Snake River basin to and including Clover Creek basin

Subregion 1705: Middle Snake: Snake River basin below Clover Creek basin to Hells Canyon Dam

Subregion 1706: Lower Snake: Snake River basin below Hells Canyon Dam to its confluence with the Columbia

LOWER COLUMBIA

Subregion 1707: Middle Columbia: Columbia River basin below the confluence with Snake River basin to Bonneville Dam

Subregion 1708: Lower Columbia: Columbia River basin below Bonneville Dam, excluding Willamette basin

COLORADO RIVER BASIN

COLORADO HEADWATERS AND THE WHITE AND YAMPA

Subregion 1401: Colorado Headwaters: Colorado River basin to but excluding Bitter Creek basin and excluding Gunnison River basin

Subregion 1405: White and Yampa River basins

UPPER GREEN

Subregion 1404: Great Divide–Upper Green: Green River basin above the confluence with Yampa River basin, and Great Divide closed basin

LOWER GREEN AND LAKE POWELL

Subregion 1406: Lower Green: Green River basin below the confluence with Yampa River basin but excluding Yampa and White River basins

Subregion 1407: Upper Colorado–Dirty Devil: Colorado River basin below the confluence with Green River basin to Lees Ferry compact point but excluding San Juan River basin

GUNNISON/DOLORES/SAN JUAN

Subregion 1402: Gunnison: Gunnison River basin

Subregion 1403: Upper Colorado–Dolores: Colorado River basin from and including Bitter Creek basin to the confluence with Green River basin

Subregion 1408: San Juan: San Juan River basin

LOWER COLORADO

Subregion 1502: Little Colorado River basin

Subregion 1504: Upper Gila: Gila River basin above Coolidge Dam, including Animas Valley closed basin

Subregion 1506: Salt River basin

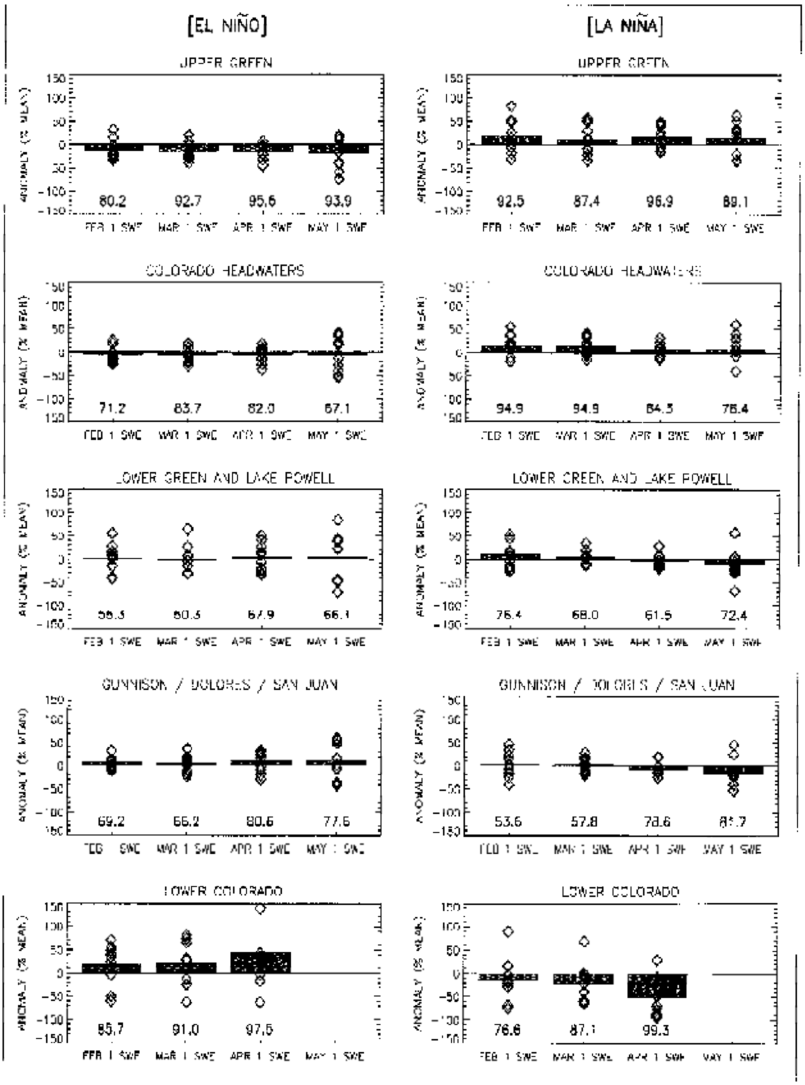

5.5 Anomalous SWE (expressed as a percentage of the mean) in El Niño and La Niña years for major subbasins in the Colorado River basin. The bars represent the mean of the ten strongest El Niño or La Niña years (based on the Niño 3.4 index; Table 5.1), and the diamonds represent the ten years used to compute the means. The April 1 SWE anomaly in the lower Colorado during the 1972–1973 El Niño event is off the scale at 216 percent of the mean (not plotted). The numbers at the bottom of each plot indicate the statistical significance of deviations as determined by a 1,000-member Monte Carlo simulation.

composite mean anomaly of the ten strongest El Niño and La Niña years (Table 5.1), and the diamonds represent the anomaly values of the individual composite members. Significance levels (in percentage) obtained from a 1,000-member Monte Carlo simulation are displayed at the bottom of each plot. Consistent with previous work (e.g., Cayan and Webb 1992), there is a general tendency for decreased SWE during El Niño years and increased SWE in La Niña years. In the broadest sense, these signals reflect displacement of the storm track by ENSO events.

Some nonlinearities are found in the association of SWE with ENSO events. In El Niño years the snowpack is very close to normal at the beginning of February, and decreases in SWE at the accumulation season are not significant at the 95 percent confidence level (Figure 5.4). Livezey et al. (1997) illustrate that although precipitation in the Pacific Northwest under El Niño conditions is below normal in October, November, February, and March, it is actually above normal in December and January, when increases in precipitation occur in conjunction with a midwinter eastward shift of the tropospheric wave train (Hoerling and Kumar 2000). Since most snow in the Pacific Northwest mountains falls in midwinter (Serreze et al. 1999), increase of precipitation in December and January largely cancels the effects of decreased precipitation in other months.

In comparison to the weak SWE signals during El Niño years, increases in SWE during La Niña years are relatively strong (often above the 95% confidence level). Stronger zonal flow over western North America under La Niña conditions steers more storm systems over the Pacific Northwest, increasing precipitation there. These increases occur throughout the winter and are particularly marked in November, December, January, and March (Livezey et al. 1997). The stronger signals in La Niña years as compared with El Niño years are consistent with the lack of symmetry in upper tropospheric circulation patterns between the extreme phases of ENSO, as mentioned previously.

ENSO-SWE Associations for the Colorado River Basin

In El Niño years, mean changes in the seasonal snowpack of the Colorado River basin (Figure 5.5) show a transition between drier-than-average conditions in the north (best expressed in the upper Green) and wetter-than-average conditions in the southwest (best expressed in the lower Colorado). Broadly opposing patterns of La Niña years are consistent with results from previous work (e.g., Cayan and Webb 1992). Signals in the upper Green (Figure 5.5) are consistent with those of the Columbia River basin (Figure 5.4), where decreases in SWE during El Niño years reflect the amplified tropospheric wave train and associated decreases in precipitation; opposite patterns appear with La Niña. In the lower Colorado basin the significant

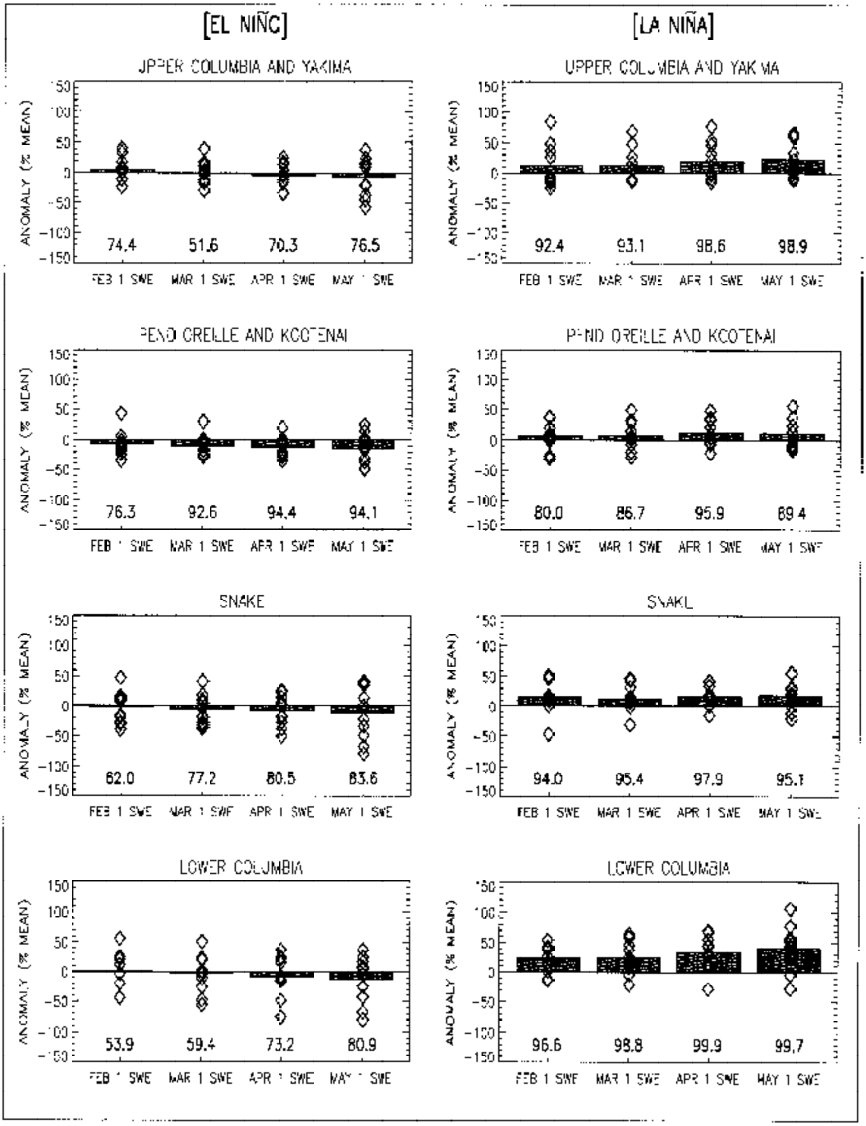

5.4 Anomalous snow-water equivalent (SWE) (expressed as a percentage of the mean) in El Niño and La Niña years for major subbasins in the Columbia River basin. The bars represent the mean of the ten strongest El Niño or La Niña years (based on the Niño 3.4 index; Table 5.1), and the diamonds represent the ten years used to compute the means. The numbers at the bottom of each plot indicate the statistical significance of deviations as determined by a 1,000-member Monte Carlo simulation.

increases in SWE in El Niño years occur in part because of the changes in precipitation associated with a strengthening of the subtropical jet; La Niña causes the reverse.

An interesting feature of Figure 5.5 is that the SWE anomalies in the lower Colorado basin increase in magnitude over the winter and tend to be much more pronounced on April 1 than on March 1. Because the mean date of maximum SWE in this region is typically near February 20 (Serreze et al. 1999), these signals reflect a prolonged accumulation season during El Niño years and early melt during La Niña years. Evidence indicates similar seasonal changes in the Colorado headwaters, the lower Green, and the San Juan River basins, but these signals are much more subdued (Figure 5.5). Sensitivity tests (not shown) demonstrate that although the signals in the lower Colorado are fairly robust, the signals in the Colorado headwaters, the lower Green, and the San Juan are sensitive to both the number of years included in the El Niño and La Niña composites and the type of index used.

DISCUSSION

Effects of ENSO on snowpack, and thus on water resources, over the Columbia River basin differ from the effects of ENSO farther south in the Colorado River basin. Over the Columbia River basin SWE generally tends to be low during El Niño years and high in La Niña years, but the trend for El Niño years is much less pronounced. Over the Colorado River basin there is a north-south transition in the effect of ENSO. Mean SWE during El Niño years is lower than average in the north and higher than average in the southwest. During La Niña years the signal is reversed. Over the lower Colorado, precipitation and SWE anomalies tend to be more pronounced in spring, when the ENSO variations have the strongest influence on regional precipitation.

Our study suggests that information on ENSO may be used to enhance seasonal hydrologic predictions in subbasins of the Columbia and Colorado River systems. In some river basins ENSO signals are weak and by themselves will provide little benefit to seasonal runoff forecasts. Our analysis shows, however, that in many instances the change in ENSO signal throughout the accumulation season is often greater than the mean ENSO signal at the end of that season. For example, SWE is high in the Colorado headwaters basin on February 1 in La Niña years but is much less so (and not significant even at the 90% level) on April 1. Because on average over two-thirds of the snowpack has accumulated by the beginning of February (Serreze et al. 1999), monitoring the water equivalent of the snowpack throughout the accumulation season and combining this information with knowledge of seasonal changes in the ENSO signal may improve predictions of water supply.

Variations in Tropical Pacific SSTs are not the only slowly varying component of the atmosphere-land-ocean system that may improve prediction of seasonal climate. Other low-frequency variations may be important, such as variations in midlatitude sea-surface temperature and continental-scale variations in land-surface snow mass, land-surface albedo, and soil moisture. For example, Gutzler and Preston (1997) show that large-scale variations in snow mass over the western United States have a significant relationship to spring and summer precipitation over New Mexico. The hypothesized mechanism, which is similar to that invoked for snow-monsoon relationships over Eurasia, is that the energy required to melt above-average snow mass and evaporate the associated higher amounts of soil moisture causes a delay in seasonal warming of the landmass. This modulates the land-ocean temperature contrast and the summer monsoonal circulation over the southwestern United States. Expansion of seasonal climate forecasts to include these additional influences may result in improved hydrologic predictions on seasonal timescales.

SUMMARY AND CONCLUSIONS

This chapter explores the utility of weather and climate information for improving intraseasonal and seasonal hydrologic predictions. We demonstrate for the Animas River in Colorado that atmospheric forecasts provide predictions of runoff with lower forecast errors than those obtained by current practice, which uses historical station data to characterize expected future weather. Because the surface hydrology of the Animas basin is dominated by snowmelt, variations in temperature are much more important than variations in precipitation for short-term runoff forecasts. Temperature forecasts are more reliable than precipitation forecasts, thereby lending enhanced accuracy to hydrologic forecasts that use output from numerical weather prediction models. In rainfall-dominated river basins, however, raw, global-scale atmospheric forecasts may be of little benefit; improvements in forecast skill may be realized only through statistical or dynamical downscaling methodologies.

For seasonal hydrologic forecasts, El Niño and La Niña events significantly modulate the seasonal snowpack evolution in many major subbasins of the Columbia and Colorado River systems. In the Columbia River basin the general tendency is for decreased SWE during El Niño years and increased SWE in La Niña years, but changes during La Niña years are much more pronounced. Over the Colorado River basin, drier-than-average conditions occur in the north and wetter-than-average conditions occur in the southwest during El Niño, and opposite trends occur during La Niña. Over the lower Colorado basin, SWE anomalies tend to be larger in spring, when the El Niño and La Niña events have the strongest influence on regional precipitation. The analysis suggests that ENSO information may be useful for improving seasonal hydrologic predictions in many subbasins of the Columbia

Hoerling, M. P., and A. Kumar. 2000. Understanding and Predicting Extratropical Teleconnections Related to ENSO. In *El Niño and the Southern Oscillation: Multi-Scale Variability and Global and Regional Impacts.* H. Diaz and V. Markgraf, eds. Cambridge University Press, Cambridge, pp. 57–88.

Hoerling, M. P., A. Kumar, and M. Zhong. 1997. El Niño, La Niña, and the nonlinearity of their teleconnections. *Journal of Climate* 10: 1769–1786.

Horel, J. D., and J. M. Wallace. 1981. Planetary scale atmospheric phenomena associated with the Southern Oscillation. *Monthly Weather Review* 109: 813–829.

Kalnay, E., M. Kanimitsu, R. Kistler, W. Collins, D. Deaven, L. Gandin, M. Iredell, S. Saha, G. White, J. Wollen, Y. Zhu, M. Chelliah, W. Ebisuzaki, W. Higgins, J. Janowiak, K-C. Mo, C. Ropeleweski, J. Wang, A. Leetmaa, R. Reynolds, R. Jenne, and D. Joseph. 1996. The NCEP/NCAR 40-year reanalysis project. *Bulletin of the American Meteorological Society* 77: 437–471.

Kalnay, E., S. J. Lord, and R. D. McPherson. 1998. Maturity of operational numerical weather prediction: Medium range. *Bulletin of the American Meteorological Society* 79: 2753–2769.

Koch, R. W., C. F. Buzzard, and D. M. Johnson. 1991. Variation of Snow Water Equivalent and Streamflow in Relation to the El Niño/Southern Oscillation. *Proceedings of the 19th Annual Meeting of the Western Snow Conference.* Juneau, Alaska, April 12–15.

Leavesley, G. H., R. W. Lichty, B. M. Troutman, and L. G. Saindon. 1983. *Precipitation-Runoff Modeling System: User's Manual.* U.S. Geological Survey Water Investigation Report 83-4238.

Leavesley, G. H., and L. G. Stannard. 1995. The Precipitation-Runoff Modeling System—PRMS. In *Computer Models of Watershed Hydrology.* V. P. Singh, ed. Water Resources Publications, Highlands Ranch, CO, pp. 281–310.

Livezey, R. E., M. Masutani, A. Leetmaa, H. Rui, M. Ji, and A. Kumar. 1997. Teleconnective response of the Pacific–North American region atmosphere to large Central Equatorial Pacific SST anomalies. *Journal of Climate* 10: 1787–1820.

Natural Resources Conservation Service (NRCS). 1988. *Snow Surveys and Water Supply Forecasting.* United States Department of Agriculture Natural Resources Conservation Service, Agricultural Information Bulletin 536.

Pulwarty, R. S. 1995. Adaptive Management of the Colorado River: The Role of Science and Scientists. In *U.S. Department of Interior Glen Canyon Environmental Studies: Aquatic, Geomorphic and Climatic Integration Group Report, Flagstaff, AZ.* T. Melis and D. Wegner, eds. U.S. Government Printing Office, Washington, DC, pp. 36–49.

Rasmusson, E. M., and J. M. Wallace. 1983. Meteorological aspects of the El Niño/Southern Oscillation. *Science* 222: 1195–1202.

Redmond, K. T., and R. W. Koch. 1991. Surface climate and streamflow variability in the western United States and their relationship to large-scale circulation indices. *Water Resources Research* 27: 2381–2399.

Seaber, P. R., F. P. Kapinos, and G. L. Knapp. 1987. *Hydrologic Unit Maps.* U.S. Geological Survey Water-Supply Paper 2294.

Serreze, M. C., M. P. Clark, R. L. Armstrong, D. A. McGinnis, and R. S. Pulwarty. 1999. Characteristics of the western U.S. snowpack from SNOTEL data. *Water Resources Research* 35: 2145–2160.

and Colorado River systems. In some basins the ENSO signals are weak and by themselves provide little benefit for seasonal runoff forecasts. In many instances, however, the change in ENSO signal during the accumulation season is greater than the mean ENSO signal at the end of that season. Therefore, monitoring the water equivalent of the snowpack during the accumulation season and combining this information with knowledge of seasonal changes in the ENSO signal may provide improved predictions of water supply.

ACKNOWLEDGMENTS

This research was supported by the NOAA Regional Assessment Program (NOAA Cooperative Agreement NA67RJ0153), the NASA RESAC Program (NAG13-99005), and a research grant from the National Science Foundation (EAR-9634329). We gratefully acknowledge comments from Martin P. Hoerling, Allan H. Frei, and Roger G. Barry.

REFERENCES

Barnston, A. G., Y. He, and D. A. Unger. 2000. A forecast product that maximizes utility for state-of-the-art seasonal climate prediction. *Bulletin of the American Meteorological Society* 81: 1271–1280.

Basist, A. N., and M. Chelliah. 1997. Comparisons of tropospheric temperatures derived from the NCEP/NCAR reanalysis, NCEP operational analyses, and the microwave sounding unit. *Bulletin of the American Meteorological Society* 78: 1431–1447.

Bjerknes, J. 1969. Atmospheric teleconnections from the equatorial Pacific. *Monthly Weather Review* 97: 163–172.

Cayan, D. R. 1996. Interannual climate variability and snowpack in the western United States. *Journal of Climate* 9: 928–948.

Cayan, D. R., and D. H. Peterson. 1990. The Influence of North Pacific Circulation on Streamflow in the West. In *Aspects of Climate Variability in the Pacific and Western Americas,* Geophysics Monograph Series, Vol. 55. D. H. Peterson, ed. American Geophysical Union, Washington, DC, pp. 375–398.

Cayan, D. R., and R. H. Webb. 1992. El Niño/Southern Oscillation and Streamflow in the Western United States. In *El Niño: Historical and Paleoclimatic Aspects of the Southern Oscillation.* H. Diaz and V. Markgraf, eds. Cambridge University Press, Cambridge, pp. 29–68.

Day, G. N. 1985. Extended streamflow forecasting using NWSRFS. *Journal of Water Resources Planning and Management* 111: 157–170.

Diaz, H. F., and C. A. Anderson. 1995. Precipitation trends and water consumption related to population in the southwestern United States. *Water Resources Research* 31: 713–730.

el-Ashry, M., and D. Gibbons. 1988. *Water and Arid Lands of the Western United States.* Cambridge University Press, New York.

Gutzler, D. S., and J. W. Preston. 1997. Evidence for a relationship between spring snow cover in North America and summer rainfall in New Mexico. *Geophysical Research Letters* 24: 2207–2210.

Trenberth, K. E. 1997. The definition of El Niño. *Bulletin of the American Meteorological Society* 78: 2771–2777.

Wilby, R. L., L. E. Hay, W. J. Gutowski Jr., R. W. Arritt, E. S. Takle, Z. Pan, G. H. Leavesley, and M. P. Clark. 2000. Hydrologic responses to dynamically and statistically downscaled General Circulation Model Output. *Geophysical Research Letters* 27: 1198–1202.

Wilby, R. L., L. E. Hay, and G. H. Leavesley. 1999. A comparison of downscaled and raw GCM output: Implications for climate change scenarios in the San Juan River basin, Colorado. *Journal of Hydrology* 225: 67–91.

Wilks, D. S. 1995. *Statistical Methods in the Atmospheric Sciences: An Introduction.* Academic Press, San Diego.